Archives of Industrial Engineering
Research Article

Prediction of Methane and Ethane Gas Hydrate Formation and Their Mixture in a Porous Medium

Talaghat MR[1*], Hariri Z[2]

[1*]Department Chemical Engineering , Shiraz University of Technology, Iran

[2]Student of Master of Science in Islamic Azad University, Shiraz Branch, Iran

Received: 10 June, 2019**; Accepted:** 21 June, 2019**; Published:** 26 June, 2019

[*]**Corresponding Author**: Talaghat MR, Department Chemical Engineering , Shiraz University of Technology, Iran. E-mail: talaghat@sutech.ac.ir

Abstract

The purpose of this paper is to study the thermodynamic modeling of the conditions for methane and ethane gas hydrate formation and their mixtures in a porous and non-porous environment. In this paper, the Van der Waals- Platteeuw thermodynamic model was used for prediction of gas hydrate formation conditions. Also, the SRK and PTV equations of state were used for calculations of driving force. In this research, the results of thermodynamic modeling in a porous were compared with the non-porous environment and laboratory data in the literature. Studies have shown that the results of the modeling are in good agreement with the laboratory data and the percentage of errors is low. The results also showed that with increasing pressure of porous and non-porous media, the equilibrium temperature increases. In addition, the effect of the pore diameter of porous media on the results of modeling was investigated for methane, ethane and their mixtures during gas hydrates formation. The results showed that by increasing the pressure for any size of the pore diameter of the porous medium, hydrate formation temperature increases. In addition, by increasing the pore diameter of the porous medium, hydrate formation temperature methane, ethane and their mixture increase at a constant pressure. The results also showed that the equilibrium temperature of the non-porous medium is higher than the equilibrium temperature of the non-porous medium. This shows that the hydrate formation in the porous medium has a deterrent effect and leads to lower temperatures and higher temperatures conditions for gas hydrate formation. The results showed that by increasing the percentage of methane in a porous or non-porous medium, the temperature of hydrate formation of the binary gas mixture of methane and ethane decreases.

Keywords: Porous Media; Thermodynamic Modeling; Gas Hydrate Formation; Van der Waals- Platteeuw Model

Introduction

Gas hydrate is a kind of nonstoichiometric clathrate crystals, formed from water and certain natural gas molecules at appropriate pressures and temperatures, which gas molecules are caged inside a network of water molecules linked together through hydrogen bonding. There are many gases that have a good structure for hydrate formation, including carbon dioxide, hydrogen sulfide, and hydrocarbons with low carbon.

Gas hydrates are formed mostly on the seabed, mostly of methane hydrate. When oil and gas components are in contact with water, three different types of hydrate networks, called I, II and H, may be formed. Each network contains a number of cavities of different sizes. In a stable hydrate, gas compounds (guest molecules) occupy a number of cavities. Type I and II structures have cavities of varying sizes, such as small and large. H structure contains holes of three different sizes, including small, medium and very large [1, 2].

Gas hydrides were discovered in 1811 by [3] during the production of chlorine gas bubbles in cold water in a laboratory. In 1832, [4] presented the first chemical formula for gas hydrates, in which a gas molecule was surrounded by ten molecules of water. In 1934, when the first gas pipeline was designed and exploited, the problem of pipe clogging by solid-gas particles of gas was introduced by Hammerschmidt in the United States [5].

Following this phenomenon, the technique of preventing the formation of this material in oil and gas pipes and the process for forming gas from the gas was formed. In 1959, the principles of thermodynamic gas hydrides were studied and explained by [6]. During the 60s and 90s, along with numerous studies on hydrates, extensive research was carried out on discovering the sources of gas hydrates in depths of the sea and Polar Regions. Since the 1990s, the United States, Japan, India, and Canada have started a long-term research program on gas hydrates with significant budget allocation. Today, attention to the phenomenon of gas hydrate and its useful and practical aspects highlights the need for further research in the following areas [1, 7]:

1. Many decades ago, there have been many quantities of natural gas stored in the gas hydrates in the ocean and Polar Regions. Given the limited resources of fossil fuels, the exploration of gas resources for energy recovery may be considered in the future.
2. The high potential of gas hydrates in the storage of natural gas makes it attractive to use it for the storage and transportation of natural gas and other gases as a competitor for liquefaction and condensation methods.
3. Gas hydrates can also be used in separation processes.

Gas gases are limited to a limited number of materials. If you want to remove a mixture of irreparable hydrates, the use of the hydrate formation feature is considered an opportunity. For example, concentrations of water-rich streams, drinking water from seawater, or separation of gas streams are mentioned.

There are two opposite directions in the studying of hydrates. While the studies related to the problematic side of hydrates, such as plugging pipeline in the oil industry, are those of trying to find ways of hydrate inhibition, there are some investigations for finding some means for the promotion of hydrate formation as a new natural energy resource and a new means for natural gas storage and transport [7,8]. But slow formation rate of natural gas hydrate has been considered to be a critical problem hindering the industrial application of gas hydrate [9]. For solving this problem,

scientists proposed for using additives such as surfactants as the strong promoters [7-10]. Surfactant (surface active agent) is compound whose molecules feature both lipophilic and hydrophilic moieties, i.e., it is amphiphilic. Molecules of surfactant in water tend to aggregate to form various kinds of supramolecular structure, such as spherical and rod-like micelles, multilayer structures and complex biological membranes [11, 12].

In recent years, researchers have reported the promotion effect of some surfactants on gas hydrate formation. Surfactant addition decreases the surface tension of the medium in which it is dissolved so that it improves the gas to liquid mass transport. Improved mass transport is believed to enable a surfactant to act as a promoter of gas hydrate formation [13]. In the absence of any additive, the hydrate appears as a thin film at the gas/liquid interface, while surfactant is present in the system hydrate crystals are seen in the vicinity of liquid-gas-solid line and in the vertical chamber walls [14, 15].

Cailletet was the first to study the gas hydrate of a binary mixture in 1877 [16]. villard was the first to discover methane, ethane and propane gas hydrates in 1888 [17, 18]. Using X-rays and numerous experiments discovered the nature of hydrate structures [18]. The porous material in gas hydrate studies can be a naturally porous material such as sand, gravel, cap rock or an artificial porous medium such as silica gel or even activated carbon.

There are many studies on the formation of gaseous hydrates in non-porous media, but research on the formation of gas hydrates in the porous medium is low and little research has been done in this area. For the first time [19] tested the methane and propane hydrate equilibrium conditions in silica gel cavities with a relative radius of 70 oA. The presence of porous material caused the pressure to form hydrate over the pressure in a free environment [20]. Measured the gas hydrate formation phase equilibrium of two parts of methane and carbon dioxide in a silica gel with Van der Waals and Platteeuw model. Anderson et al. examined methane, carbon dioxide, methane-carbon dioxide hydrates in a silica gel environment [21].

Turner and colleagues in 2005 showed that there is no difference between the fuzzy hydrate equilibrium in the non-porous medium and the porous medium with a cavity size distribution of more than 600 angstroms [22]. Concluded that by decreasing the diameter of porous media, the prevention conditions of this environment increase, due to increased capillary effect and reduced water activity. They also found that energy between the water surface and hydrate can be attributed to changes in temperature and type of hydrate structure and occupancy of transplanted cavities [23, 24]. The effect of operational conditions on performance of solid desiccant based hybrid cooling system in hot and humid climate was estimated [24]. They also studied the performance analysis of a solid desiccant assisted hybrid space cooling system using TRNSYS [25].

In this paper, gas hydrate formation conditions for methane, ethane and their mixtures in a porous and non-porous environment is studied using Van der Waals and Platteeuw thermodynamic model.

Thermodynamic modeling

Several thermodynamic models have been proposed to calculate the gas hydrate phase equilibrium properties, all of which are based on the Van der Waals and Platteeuw statistical theory of dynamic.

This theory provides an equation for the difference in chemical potential in a water-free and water-rich hydrate network. The difference in the chemical potential of water in the empty phase and hydrate is calculated by (Equation 1)

$$\Delta\mu_w^{\beta-H} = RT\sum_{m=1}^{n.cavity}\nu_m \ln\left(1+\sum_{i=1}^{nc}C_{mi}f_i\right) \quad (1)$$

In the above equation, V_m is the number of m type holes per water molecule in the crystalline hydrate network, C_{mi} is the Langmuir coefficient i in the cavity of the type m, n_c is the number of gas components that can enter the hydrate network, and f_i is the fugacity of the guest molecules in the hydrate phase, which is calculated by the equation of state. Langmuir constant is calculated from the (Equation 2) according to Lenard-Jones's theory:

$$C_{mi} = \frac{4\pi}{kT}\int_0^{\tilde{R}_m-a_i}\exp\left(\frac{-\omega_{mi}(r)}{kT}\right)r^2dr \quad (2)$$

In the above equation, k is the Boltzmann constant, and ω(r) is the spherical potential function. In (Equation 2) it is seen that the Langmuir coefficient is a temperature function. To calculate the spherical potential function, the Kihara energy potential function is used according to (Equation 3).

$$\Gamma(r) = 4\varepsilon\left[\left(\frac{\sigma}{r-2a}\right)^{12}-\left(\frac{\sigma}{r-2a}\right)^{6}\right] \quad (3)$$

In the above equation, σ is collision diameter, a is hard core radius, and ε is depth of energy well. The spherical potential function is also calculated by (Equation 4).

$$\omega(r) = 2z\varepsilon\left[\frac{\sigma^{12}}{\tilde{R}^{11}r}\left(\delta^{10}+\frac{a}{\tilde{R}}\delta^{11}\right)-\frac{\sigma^{6}}{\tilde{R}^{5}r}\left(\delta^{4}+\frac{a}{\tilde{R}}\delta^{5}\right)\right] \quad (4)$$

In the above equation, Z is the neighborhood of each cavity, R is the mean radius of the cavity, and δ^N is calculated by (Equation 5):

$$\delta^N = \frac{1}{N}\left[\left(1-\frac{r}{\tilde{R}}-\frac{a}{\tilde{R}}\right)^{-N}-\left(1+\frac{r}{\tilde{R}}-\frac{a}{\tilde{R}}\right)^{-N}\right] \quad (5)$$

N can select values 4, 5, 10 and 11. The optimized values of the Kihara potential function constants for a number of gas compounds are available in the literature [8]. The optimized values of the constants of the Kihara potential function for a number of gas compounds are given in (Table 1) [12]. The fugacity coefficients are also calculated using SRK and PTV equations of state [10, 9].

Table (1) Kihara potential constants [1]

component	$\frac{\varepsilon}{k}(K)$	$\sigma(A^o)$	$a(A^o)$
Methane	3.14393	593.155	0.3834
Ethane	3.24693	188.181	0.5651
Propane	3.41670	192.855	0.6502

The difference in the chemical potential of water in the liquid phase and the empty hydrate network is calculated by (Equation 6):

$$\frac{\Delta\mu_w^{\beta-l}}{RT} = \frac{\Delta\mu_w^{0}}{RT_0}-\int_{T_0}^{T}\frac{\Delta h_w^{\beta-l}}{RT^2}dT+\int_0^P\frac{\Delta v_w^{\beta-l}}{RT}dP-\ln(a_w) \quad (6)$$

In the above equation, T is freezing point of water (in absolute temperature), $\Delta\mu_w^0$ is the difference in the chemical potential of water in the liquid phase and the empty hydrate network at 273.153 K and zero pressure, $\Delta h_w^{\beta-l}$ is the molar enthalpy difference between the liquid phase and the empty hydrate network, $\Delta v_w^{\beta-l}$ is molar volume difference the liquid phase and the empty hydrate network. (Equation 7) is obtained by putting the (Equation 6) in the (Equation 1).

$$\frac{\Delta\mu_w^0}{RT_0}-\int_{T_0}^{T}\frac{\Delta h_w^{\beta-l}}{RT^2}dT+\int_0^P\frac{\Delta v_w^{\beta-l}}{RT}dP-\sum_{m=1}^{n.cavity}\nu_m\ln\left(1+\sum_{i=1}^{nc}C_{im}f_i\right)-\ln(a_w)=0 \quad (7)$$

The difference in the gas hydrate formation in a porous medium with a non-porous medium is related to water activity. The water activity for a non-porous medium is obtained from the f (Equation 8) for a pure water value [5-7].

$$a_w=\gamma_w x_w \quad (8)$$

X_w is the composition of the water percentage in the liquid phase and γ_w is the water activity coefficient. x_w is calculated by (Equation 9):

$$x_w=1-\sum_k x_k \quad (9)$$

At low concentrations, the solubility of the k component in the liquid phase and atmospheric pressure is calculated by Henry's law (Equation 10). Also, the x_k and Henry's constant are calculated, by (Equation 11-12).

$$H_{kw}=\frac{1}{x_k(T)} \quad (10)$$

$$R\ln x_k=H_{kw}^0+\frac{H_{kw}^1}{T}+H_{kw}^2\ln T+H_{kw}^3T \quad (11)$$

$$-\ln\frac{H}{101325}=H_{kw}^0+\frac{H_{kw}^1}{T}+H_{kw}^2\ln T+H_{kw}^3T \quad (12)$$

At higher pressures, the Henry's constant of component k is calculated from (Equation 13):

$$H_{kw}(T)\frac{V_k^\infty}{}(P-P_{sw})=\ln H_{kw}(T,P) \quad (13)$$

V_K^∞ is the partial molar volume at infinity of water dilution, H is Henry's constant and Psw is the saturation pressure of water.

The activity of water in a porous medium is calculated from the (Equation 14):

$$\ln(a_w)_{pore}=\ln(a_w)-\frac{v_L F\sigma_{HW}\cos\theta}{rRT} \quad (14)$$

In the equation above, F is the shape factor, σ_{HW} is interfacial energy, r is the average radius of the cavities and θ is the wetting angle. The interfacial energy is calculated by (Equation 15).

$$\sigma_{HW}=\frac{a+bT}{1+\frac{\delta}{r}} \quad (15)$$

In the above equation, a and b are constant values whose values are available in the literature [6]. For more information, see (Table 2) [11].

Table (2): Constants for interfacial energy (Equation 15) [23]

component	a (J/m^2)	b ($J/m^2.k$)
methane	0.0102	-0.00024
multicomponent	0.7669	-0.00026

Results and discussion

In this paper, in order to predict the gas hydrate formation in a porous medium, the thermodynamic model of van der Waals and Platteeuw is used. To evaluate the model, the results of this modeling were compared for a porous medium and non-porous medium with valid laboratory data in the literature. Furthermore, to study the effect of different state equations on the prediction of hydrate formation conditions, two equations of state SRK and PTV were used. The

predicted methane equilibrium temperature during hydration formation in a porous medium (such as silica gel) with 6 and 10 nm pores size and non-porous media using the SRK and PTV equations of state was compared with [20,23]. laboratory data in the same conditions, respectively.

Table (3): Comparison between predicted methane equilibrium temperature during hydrate formation in porous media (with 6 nm pores size) and non-porous media with seo et al. laboratory data [20].

AAD% PTV equation of state	AAD% SRK equation of state	Calculated temperature for non-porous media (K)	Calculated temperature for porous media (K) PTV	Calculated temperature for porous media (K) SRK	Measured temperature porous media (K)	Pressure (bar)
3.35	3.13	280.17	266.09	266.67	275.30	51.7
2.80	2.74	281.96	268.91	269.07	276.65	61.9
2.55	2.49	283.41	270.86	271.04	277.95	72
2.41	2.35	284.71	272.61	272.78	279.35	82.75
2.10	2.04	285.81	274.06	274.22	279.95	93.26
1.96	1.78	287.15	275.46	275.95	280.95	105

Table (4): Comparison between predicted methane equilibrium temperature during hydrate formation in porous media (with 10 nm pore size) and non-porous media with Zarifi et al. laboratory data [23].

AAD% PTV equation of state	AAD% SRK equation of state	Calculated temperature for non-porous media (K)	Calculated temperature for porous media (K) PTV	Calculated temperature for porous media (K) SRK	Measured temperature porous media (K)	Pressure (bar)
0.12	0.4316	277.93	274.38	275.70	274.47	41.40
0.09	0.4223	278.10	274.55	275.80	274.64	42.10
0.11	0.2182	278.45	274.96	275.60	275.00	43.60
0.06	0.3889	278.59	275.05	276.20	275.13	44.20
0.04	0.2934	279.55	276.00	276.90	276.09	48.60
0.32	0.6437	279.97	276.42	278.30	276.52	50.70
0.11	0.2169	280.05	276.95	277.20	276.60	51.10
0.07	0.2566	280.15	276.59	277.40	276.69	51.60
0.01	0.5451	280.46	276.90	278.50	276.99	53.20

Table (5): Comparison between predicted methane equilibrium temperature during hydrate formation in porous media (with 30 nm pore size) and non-porous media with Achida et al. laboratory data using the SRK and PTV equations of state [26].

Pressure (bar)	Measured temperature for porous media (K)	Calculated temperature for porous media (K) SRK	Calculated temperature for porous media (K) PTV	Calculated temperature for non-porous media (K)	AAD% SRK Equation of state	AAD% SRK Equation of state
50	278.20	277.64	277.53	279.83	0.20	0.24
59	279.50	279.38	279.26	281.48	0.04	0.08
56	279.70	278.84	278.72	280.97	0.31	0.35
70	280.60	281.14	281.01	283.14	0.19	0.15

The results of this study are presented in (Tables 3-4), respectively. Also, (Table 5) shows the comparison of the results of modeling with the results of laboratory data of Achida et al. in porous media with 30 nm pores size. As shown in (Tables 3-5), increasing the pressure in a porous or non-porous medium increases the equilibrium temperature of methane hydrate formation, and this increase in the non-porous medium is more than a porous medium.

This suggests that the formation of hydrate in the porous medium plays a deterrent role and the equilibrium conditions lead to lower temperature and higher pressure. The results also showed that this thermodynamic model can well predict the formation of hydrate conditions in porous and non-porous media. It is also observed that the calculated error between the modeling results obtained by using different equations of state laboratory data is low, so this model can well predict the methane hydrate formation conditions. Further, the results show that, in general, the percentage error of the SRK equation of state is less than the PTV equation of state for prediction of methane gas hydrate equilibrium temperature.

For more information, the comparison between equilibrium curve methane hydrate formation conditions in porous media, non-porous media and Seo et al. experimental data was shown in (Figure 1). (Figure 1) shows that at a certain pressure, the hydrate formation temperature in a non-porous medium is higher than that of the experimental data of Seo et al. and the porous medium. The results also show that the model predicts the gas hydrate formation temperature in less experimental data.

Also, in this research, the results of this modeling were compared with the results of laboratory data of Zarifi et al., and Seo et al. for a porous medium with 15 nm pore size. These results are presented in (Tables 6-7), respectively. By observing the tables, it turns out that the results are quite similar for porous media with a pore size of 10 and 15 nm. In addition, by studying these tables, it is observed that by reducing the pore diameter of the porous medium, the hydrate formation process becomes more difficult and the error between experimental results and modeling is increased. This is due to increased capillary effect and reduced water activity.

Figure (1): Comparison between equilibrium curve methane hydrate formation conditions in porous media, non-porous media and Seo et al. experimental data

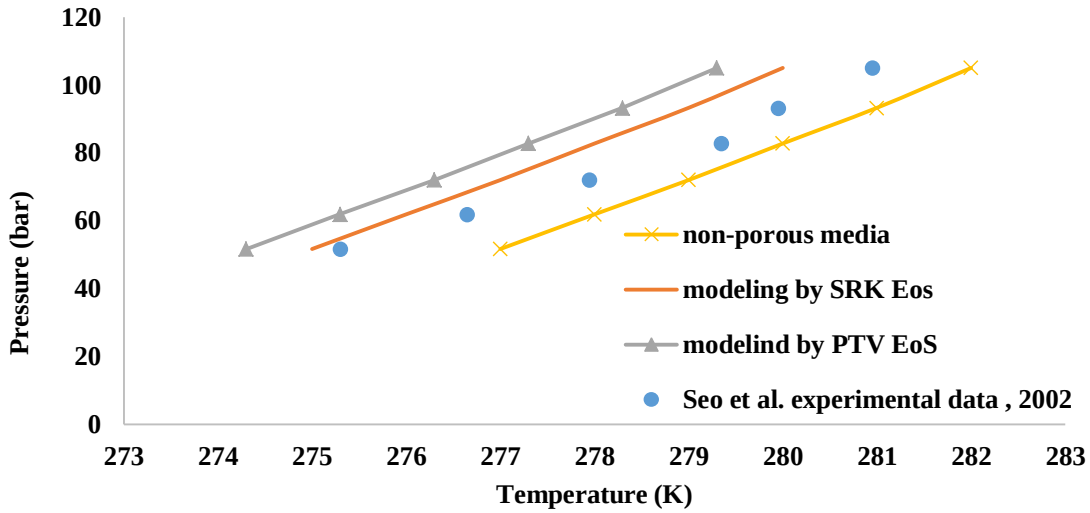

Table (6): Comparison between predicted methane equilibrium temperature during hydrate formation in porous media (with 15 nm pores size) and non-porous media with Zarifi et al. laboratory data using the SRK and PTV equations of state [23].

Pressure (bar)	Measured temperature for porous media (K)	Calculated temperature for porous media (K) SRK	Calculated temperature for porous media (K) PTV	Calculated temperature for non-porous media (K)	AAD% SRK Equation of state	AAD% SRK Equation of state
33	273.30	273.28	273.21	275.58	0.0077	0.0343
40.5	275.10	275.40	275.31	277.70	0.1075	0.0768
48.2	277.00	277.16	277.07	279.47	0.0593	0.0251
55.5	278.30	278.57	278.47	280.88	0.0994	0.0623
Total average percentage error					0.0684	0.0496

Table (7): Comparison between predicted methane equilibrium temperature during hydrate formation in porous media (with 15 nm pores size) with Seo et al. laboratory data using the SRK and PTV equations of state [20].

Pressure (bar)	Measured temperature for porous media (K)	Calculated temperature for porous media (K) SRK	Calculated temperature for porous media (K) PTV	AAD% SRK equation of state	AAD% PTV equation of state
48.25	277.15	277.17	277.08	0.0089	0.0252
60.60	279.15	279.44	279.33	0.1038	0.0658
71.60	280.45	281.05	280.94	0.2133	0.1744
82.43	281.75	282.37	282.26	0.2185	0.1810
92.75	282.88	283.44	283.34	0.1964	0.1627
102.85	273.70	284.35	284.27	0.2771	0.1996
Total average percentage error				0.1696	0.1347

In addition, the conditions for the formation of ethane hydrates in a porous and non-porous environment were also investigated and the effect of pore size of porous media on the equilibrium temperature of hydrate formation was studied. The results of this study are presented in (Table 8). As seen from (Table 8), the temperature of the hydrate formation increases with increasing pressure for any size of the pore diameter of the porous medium. It is also observed that the hydrate formation temperature of ethane in the non-porous medium is higher than the hydrate formation temperature in the porous medium. It is also observed that at constant pressure with increasing pore size, the formation temperature of hydrate increases. It also shows that by increasing the size of the cavity, the porous medium is more similar to the non-porous medium and decreases the role of deterioration of the porous medium.

Table (8): Effect of the pore size on the ethane hydrate formation in a porous media

Calculated temperature for non-porous media (K)	Calculated temperature for porous media (K) pore size (30 nm)	Calculated temperature for porous media (K) pore size (15 nm	Calculated temperature for porous media (K) pore size (10 nm)	Pressure (bar)
278.90	286.29	284.55	282.65	10
293.32	292.00	290.56	289.00	20
296.14	294.96	293.63	292.28	30
297.75	296.62	294.21	292.83	40

Also, the conditions for propane gas hydrate formation in a porous media were investigated.

The results for comparison between predicted propane equilibrium temperature during hydrate formation in porous media with 10 nm and 15 nm pore size, non-porous media and Li et al. experimental data was shown in (Tables 9-10), respectively [26]. The effect of pore size of porous media on the prediction of propane hydrate formation was studied. The results of this study are shown in (Figure 2).

Table (9): Comparison between predicted propane equilibrium temperature during hydrate formation in porous media (with 10 nm pores size) and non-porous media with Li et al. Experimental data [27].

Pressure (bar)	Experimental data (K)	Calculated Temperature (K) Using SRK EoS	Calculated Temperature (K) Using PTV EoS	Equilibrium Temperature (K) Non- porous media	AAD% using SRK EoS	AAD% using PTV EoS
2.01	263	264.38	264.37	274.83	0.5247	0.5214
3.19	269.5	266.96	266.94	276.94	0.9419	0.9471

Table (10): Comparison between predicted propane equilibrium temperature during hydrate formation in porous media (with 15 nm pores size) and non-porous media with Li et al. Experimental data [27].

Pressure (bar)	Experimental data (K)	Calculated Temperature (K) Using SRK EoS	Calculated Temperature (K) Using PTV EoS	Equilibrium Temperature (K) Non- porous media	AAD% using SRK EoS	AAD% using PTV EoS
1.75	264.2	267.56	267.55	274.19	1.27	1.26
3.26	271.2	270.78	270.77	277.03	0.1528	0.1577

Figure (2): Effect of pore size on the propane hydrate formation conditions in porous media

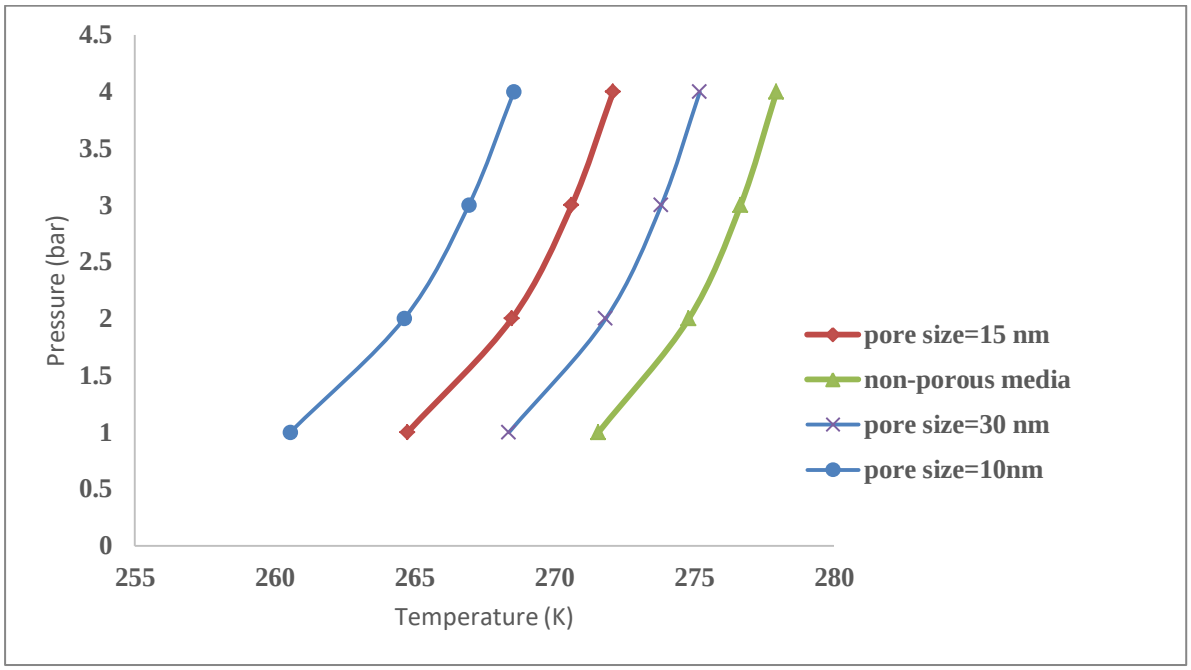

Also, in this study, the conditions for the formation of binary mixtures of methane and ethane in a porous medium have been investigated. The results of this study are compared with a non-porous medium. The results of this study are shown in (Table 11). By observing (Table 11), it is shown that with increasing methane percentage, the gas hydration formation temperature of this binary gas mixture is reduced for porous or non-porous medium. Conversely, by increasing the percentage of ethane in this gas binary mixture, its gas hydrate formation temperature increases.

This indicates that ethane plays a more important role in increasing the hydrate formation temperature. It is also observed that for this gas binary mixture, the gas hydrate formation temperature for a porous medium is lower than the hydrate formation temperature for a non-porous medium. These results are seen in (Figure 3). This figure shows the comparison between the calculated temperature of the gas hydrate formation conditions of the binary gas mixture including methane and ethane at a constant pressure of 10 bar in a non-porous medium and in a porous medium with a size of 10 nm.

Moreover, the conditions for the formation of binary mixtures of propane with methane or ethane in a porous medium have been investigated. The results of this study are compared with a non-porous medium.

The results are shown in (Figure 4-5), respectively. These figures show that at a certain pressure, the hydrate formation temperature in a non-porous medium is higher than that the porous medium.

Table (11): Hydrate formation temperature of binary mixture of methane and ethane in a porous medium with 10 nm pores size and a pressure of 10 bar

CH_4%	Calculated temperature for porous media (K)	Calculated temperature for non-porous media (K)
10	282.30	287.52
20	281.73	286.98
30	280.97	286.28
40	279.97	285.39
50	278.92	284.29
60	277.10	282.98
70	274.97	281.05
80	271.94	278.47
90	266.99	274.31
100	252.23	287.52

Figure (3): Comparison between prediction of hydrate formation temperature for methane and ethane binary mixture at 10 bar pressure in porous media (with pore diameter of 10 nm) and non-porous media

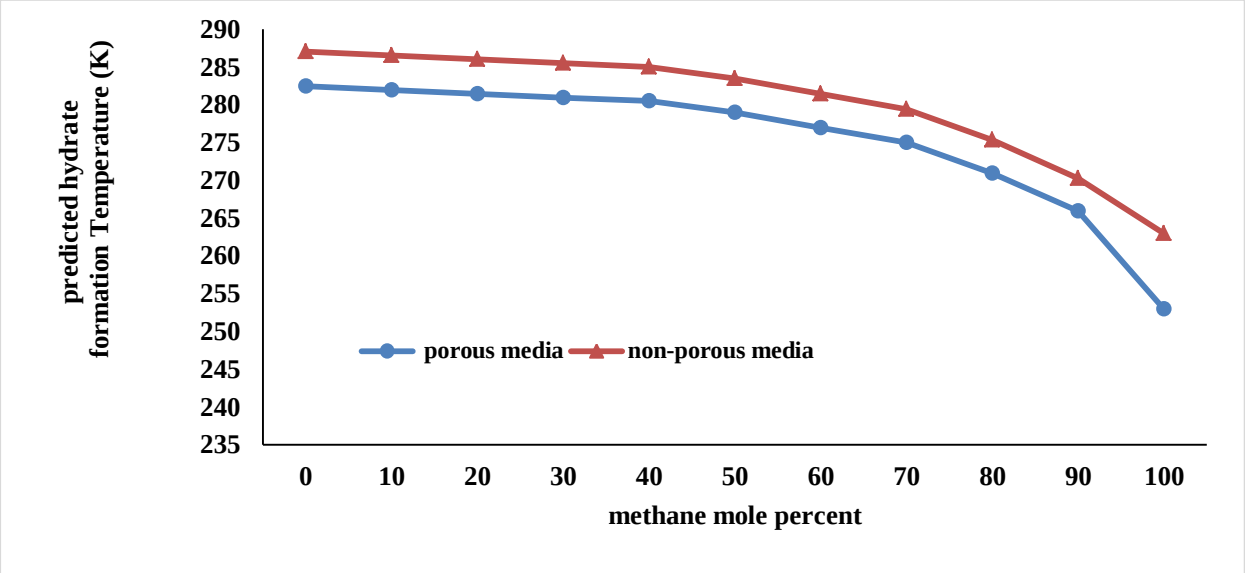

Figure (4): Comparison between prediction of hydrate formation condition for methane and propane binary mixture in porous and non-porous media with equal composition percentage

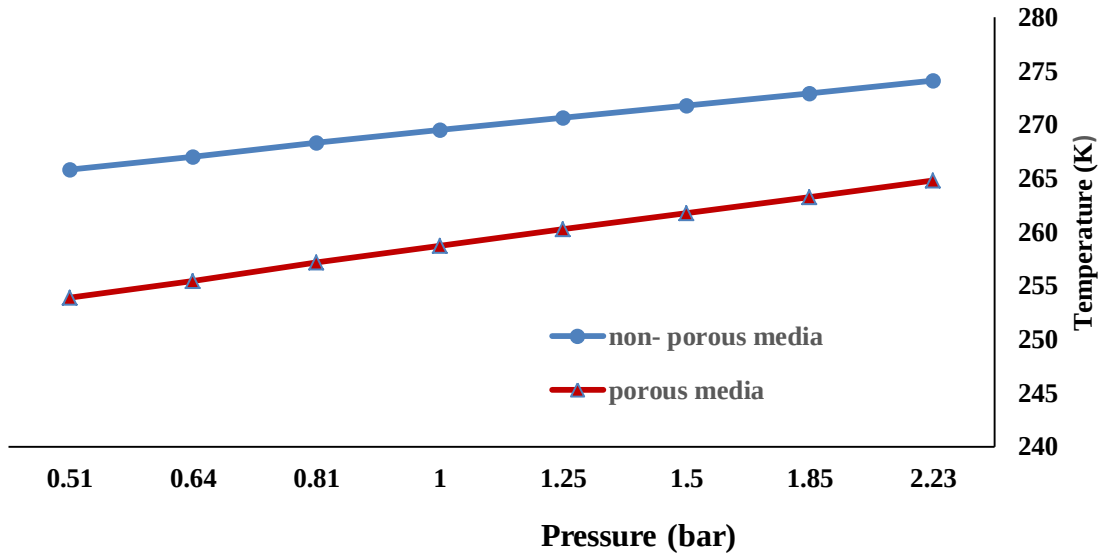

Figure (5): Comparison between prediction of hydrate formation condition for ethane and propane binary mixture in porous and non-porous media with equal composition percentage

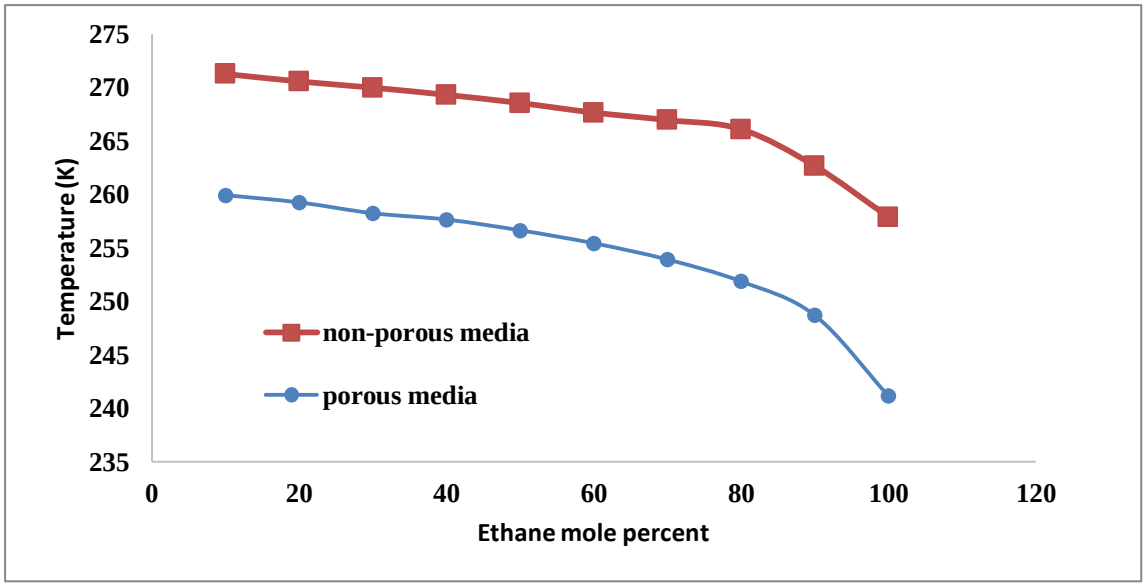

The results also show that the model predicts the gas hydrate formation temperature in less experimental. This suggests that the formation of hydrate in the porous medium plays a deterrent role. In this research, equilibrium gas hydrate temperature of the ternary gas mixture including methane, ethane, and propane, in porous media at various pore size was studied. Comparison between the predicted of equilibrium gas hydrate temperature of the ternary gas mixture including 93.25% methane, 4.75% ethane and 2% propane, in porous media (with 10 nm pores size) and Zarifi et al. experimental data for the structure I and II are presented in (Table 12). (Table 13) shows the same results for 15 nm pores size using SRK and PTV equations of

state. As shown in (Tables 10-11), increasing the pressure in a porous or non-porous medium increases the equilibrium temperature of hydrate formation, an increase in temperature in the non-porous environment is more than a porous medium.

This suggests that the formation of hydrate in the porous medium has a deterrent effect and causes the formation of hydrate to lower temperatures and high pressures. The results also showed that this thermodynamic model can well predict the gas hydrate formation conditions in porous and non-porous media. It is also observed that the results obtained using different equations of state have little error than laboratory data. In addition, the effect of pore size on the hydrate formation conditions of the ternary mixture of methane, ethane, and propane with the percentage of equal composition in porous media was studied. The results were shown in (Figure 6). This figure shows that at a certain pressure, the hydrate formation temperature decreases with increasing pore size. As the diameter of the pores decreases, resistance to hydrate formation increases.

Table (12): Comparison between the predicted of equilibrium hydrate temperature of ternary gas mixture including 93.25% methane, 4.75% ethane and 2% propane, in porous media (with 10 nm pores size) and Zarifi et al. experimental data for structure I and II[23].

AAD% for structure II	AAD% for structure I	Calculated equilibrium temperature (K) for structure II	Calculated equilibrium temperature (K) for structure I	Experimental data (K)	Pressure (bar)
0.5017	0.5644	283.92	280.91	282.50	56.7
0.6789	0.4868	281.60	278.34	279.60	43.6
0.6714	0.4952	281.58	278.32	279.70	43.5
0.6173	0.5154	Total Average Percentage Error			

Table (13): Comparison between the predicted of equilibrium hydrate temperature of ternary gas mixture including 93.25% methane, 4.75% ethane and 2% propane, in porous media (with 15 nm pores size) and Zarifi et al. experimental data using SRK and PTV EoS [23]

AAD% using PTV EoS	AAD% using SRK EoS	Equilibrium Temperature (K) Non- porous media	Calculated Temperature (K) Using PTV EoS	Calculated Temperature (K) Using SRK EoS	Experimental data (K)	Pressure (bar)
0.3319	0.3522	282.36	278.47	278.42	279.40	35.30
0.3659	0.3922	285.07	281.47	281.39	282.50	48.00
0.2875	0.3183	286.71	283.28	283.20	284.10	58.40
0.2989	0.3316	287.22	283.85	383.80	284.70	62.20
0.3210	0.1742					

Figure (6): Effect of pore size on the hydrate formation conditions of ternary mixture of methane, ethane and propane with percentage of equal composition in porous media

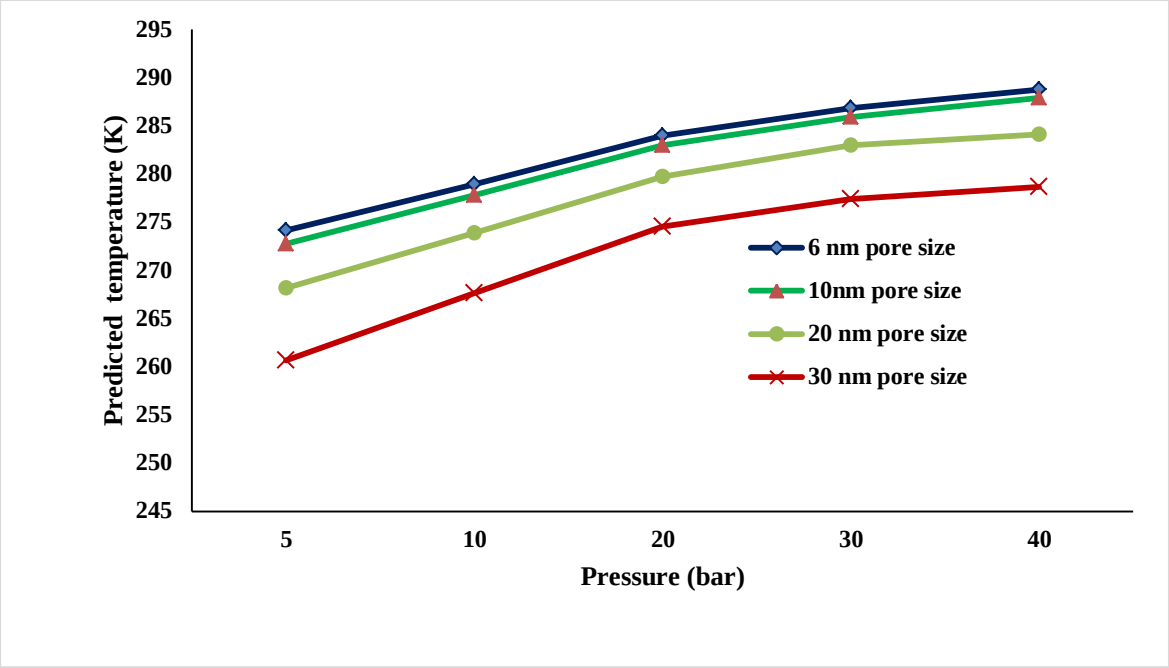

Conclusion

- By reducing the pore diameter of the porous medium, the hydrate formation process becomes more difficult and the error between the experimental results and modeling is increased. This is due to increased capillary effect and reduced water activity.
- The power of prediction for pores with a smaller radius decreases, due to increased capillary effect and increased pressure for hydrate formation.
- The equilibrium temperature prediction showed that the SRK equation has a lower error than the PTV equation.
- The results showed that at a constant pressure the hydrate formation temperature in the non-porous environment was higher than the porous medium
- By increasing methane percentage, the gas hydration formation temperature of this binary gas mixture is reduced for porous or non-porous medium.

List of nomenclatures:

a	Hard core radius; m
a	constant value in Eq. (17)
b	constant value in Eq. (17)
C_{mi}	The Langmuir coefficient i in the cavity of the type m
f_i	Fugacity of component i
F	Shape factor
H_{kw}	Henry's constant
k	Boltzmann constant
N	constant value: can select values 4, 5, 10 and 11in Eq. (5)
n_c	Number of gas components that can enter the hydrate network

r	Average radius of the cavities in Eq. (14); m
R	Universal gas constant
$\tilde{R}$	the mean radius of the cavity in Eq. (4); m
P_{sw}	Saturation pressure of water, bar
T	Temperature; K
T	Freezing point of water in Eq. (6); K
$\Delta h_w^{\beta-l}$	Molar enthalpy difference between the liquid phase and the empty hydrate network(Joule/mol)
$\Delta\mu$	Chemical potential difference (Joule/mol)
$\Delta\mu_w^0$	Difference in the chemical potential of water in the liquid phase and the empty hydrate network at 273.153 K and zero pressure (Joule/mol)
$\Delta v_w^{\beta-l}$	Molar volume difference the liquid phase and the empty hydrate (cm^3/mol)
V_m	Number of m type holes per water molecule in the crystalline hydrate network
V_K^∞	Partial molar volume at infinity of water dilution(cm^3/mol)
X_w	Composition of the water percentage in the liquid phase
Z	The neighborhood of each cavity

Greek symbols

θ	Wetting angle
$\omega(r)$	Spherical potential function
σ	Collision diameter
σ_{HW}	Interfacial energy in Eq. (14)
ε	Depth of energy well
γ_w	Water activity coefficient

Reference

1. Sloan ED, Koh CA (2007) Clathrate Hydrates of Natural Gases, 3rd ed.; CRC Press (Taylor and Francis Group): Boca Raton, FL.
2. Carroll J (2002) Natural Gas Hydrate, Elsevier Science & Technology Books.
3. Davy H (1811) "The Bactrian Lecture: On some of the combinations of oxy muriatic gas and oxygen, and on the chemical relations of these principles, to inflammable bodies", Philosophical Transactions of the Royal Society of London. The Royal Society; 101: 1-35.
4. Faraday F (1823) On fluid chlorine, Philosophical Transactions of the Royal Society of London. The Royal Society; 113: 160–165.
5. Hammerschmidt EG (1935) "Formation of Gas Hydrates in Natural Gas Transmission Lines," Ind. Eng. Chem.; 26(8): 851–855.
6. Van der Waals JH, Platteeuw JC (1958) Clathrate solutions, Advances in Chemical Physics Bd.2, Interscience Publisher, Inc., New York; 1-57.
7. Sun ZG, Wang R, Ma RS, et al. (2003) Natural gas storage in hydrate with the presence of promoters, Energ. Convers. Manage.; 44(17): 2733-2742.
8. Karaaslan U, Parlaktuna M (2000) Surfactants as hydrate promoters?. Energ. Fuel; 14(5), 1103-1107.
9. Ganji H, Manteghian M, Sadaghianizadeh K, et al. (2007) Effect of different surfactants on methane hydrate formation rate, stability and storage capacity, Fuel; 86(3): 434-441.
10. Zhang CS, Fan SS, Liang DQ, et al. (2004) Effect of additives on formation of natural gas hydrate, Fuel; 83(16): 2115-2121.
11. Smith LA, Duncan A, Thomson GB, et al. (2004) Crystallisation of sodium dodecyl sulphate from aqueous solution: phase identification, crystal

morphology, surface chemistry and kinetic interface roughening, J. Cryst. Growth; 263(1-4): 480-490.
12. Di Profio P, Arca S, Germani R, et al. (2005) Surfactant promoting effects on clathrate hydrate formation: Are micelles really involved?. Chem. Eng. Sci.; 60(15): 4141-4145.
13. Yoslim J, Englezos P (2008) The effect of surfactant on the morphology of methane/propane clathrate hydrate crystals, Proceedings of the 6th International Conference on Gas Hydrate (ICGH 2008), Vancouver, British Columbia, CANADA.
14. Gayet P, Dicharry C, Marion G, et al. (2005) Experimental determination of methane hydrate dissociation curve up to 55 Mpa by using a small amount of surfactant as hydrate promoter, Chem. Eng. Sci.; 60(21): 5751-5758.
15. Lee JD, Song M, Susilo R, et al. (2006) Dynamics of methane-propane clathrate hydrate crystal growth from liquid water with or without the presence of n-heptane, Crys. Growth Des.: 6: 1428-1439.
16. Cailletet L (1877) "Sur la liquéfaction de l'acétylène" C. R.; 85: 851-951.
17. Villard MP (1888) "Sur quelques nouveaux hydrates de gaz Comptes Rendus de l'Académie des Sciences (in French); 106: 1602-1603.
18. Von Stackelberg M, Müller HR, Feste (1954) Gas Hydrate II, Zeitschrift fuer Elektrochem; 58: 25-31.
19. Handa YP, Stupin DJ (1992) Thermodynamic properties and dissociation characteristics of methane and propane hydrate in 70-A- radius silica gel pores. J. Phys. Chem.; 96(21): 8599-8603.
20. Seo Y, Lee H, Uchida T (2002) Methane and Carbon Dioxide Hydrate Phase Behavior in Small Porous Silica Gels Langmuir; 18(24): 9164-9170.
21. Anderson R, Llamedo M, Tohidi B, et al. (2003) "Experimental Measurement of Methane and carbon dioxide clathrate hydrate equilibria in mesoporous silica" J. Phys. Chem.; 107(): 3507-3514.
22. Turner DJ, Cherry RS, Sloan ED (2005) "Sensitivity of methane hydrate phase equilibria to sediment pore size", Fluid Phase Equilib; 228-229: 505-510.
23. Zarifi M, Javanmardi J, Hashemi H, et al. (2016) Experimental Study and Thermodynamic Modelling of Methane and Mixed C1 + C2 + C3 Clathrate Hydrates in the Presence of Mesoporous Silica gel, Fluid Phase Equilibria,; 423: 17-24.
24. Jani DB, Mishra M, Sahoo PK (2018) Investigations on effect of operational conditions on performance of solid desiccant based hybrid cooling system in hot and humid climate. Thermal Science and Engineering Progress; 7: 76-86.
25. Jani DB, Mishra M, Sahoo PK (2018) Performance analysis of a solid desiccant assisted hybrid space cooling system using TRNSYS. Journal of Building Engineering; 19: 26-35.
26. Achida T, Ebinuma T, Takeya S, et al. (1999) Dissociation Condition Measurements of Methane Hydrate in Confined Small Pores of Porous Glass. J. Phys. Chem.; 103: 3659-3662.
27. Li XS, Zhang Y, Li G, et al. (2008) Gas hydrate equilibrium dissociation conditions in porous media using two thermodynamic approaches. J. Chem. Thermodyn; 40(9): 1464-1474.

***Citation*:** Talaghat MR, et al., (2019), "Prediction of Methane and Ethane Gas Hydrate Formation and Their Mixture in a Porous Medium". Arch Ind Engg; 2(1): 1-16.

DOI **10.31829/2637-9252/aie2019-2(1)-109**